Contents lists available at ScienceDirect

Translational Oncology

Tumor-targeting anti-EGFR x anti-PD1 bispecific antibody inhibits EGFR-overexpressing tumor growth by combining EGFR blockade and immune activation with direct tumor cell killing

Li Li[1], Lan Deng[1], Xiaoqing Meng, Changling Gu, Li Meng, Kai Li, Xuesai Zhang, Yun Meng, Wei Xu, Le Zhao, Jianhe Chen, Zhenping Zhu*, Haomin Huang*

Sunshine Guojian Pharmaceutical (Shanghai) Co. Ltd. a 3SBio Inc. Company, 399 Libing Road, Shanghai 201203, China

ARTICLE INFO

ABSTRACT

We developed a strategy to combine conventional targeted therapy with immune checkpoint blockade using a tumor-targeting bispecific antibody (BsAb) to treat solid tumors. The BsAb was designed to simultaneously engage a tumor-associated antigen, epidermal growth factor receptor (EGFR), and programed cell death protein 1 (PD1). In addition to its direct anti-tumor activity via EGFR inhibition, the BsAb mediated efficient antibody-dependent cellular cytotoxicity (ADCC) and activated T cell antitumor im munity through blockade of PD1 from interacting with its counterpart, programed cell death ligand 1 (PDL1). Further, the BsAb exhibited a potent direct tumor cell killing activity in the presence of PBMC, most likely, via activating and, at the same time, physically engaging T cells with tumor cells. Taken together, we here illustrate a new strategy in the design and production of novel BsAbs with enhanced therapeutic efficacy through both direct tumor growth inhibition and T cell activation via tumor-targeted immune checkpoint blockade.

Introduction

Tumor growth and metastasis are strongly influenced by tumor microenvironment. Within the tumor microenvironment, T cells, B cells, natural killer (NK) cells, tumor-associated macrophage (TAM), dendritic cells (DC), myeloid-derived suppressor cells (MDSC) and other cells form a dynamic immune network [1,2]. Cancer cells can dampen, change and block the anti-tumor activities of immune cells, a mechanism called immune evasion. Programmed cell death protein 1/ programed cell death ligand 1 (PD1/PDL1), an immune checkpoint complex, exploited by many tumors to evade immune system, has been extensively studied. Binding of PD1 to PDL1 (CD274, B7-H1) suppresses the function of tumor-infiltrating T-lymphocytes, by inducing apoptosis or turning them into a state of exhaustion [3]. In addition, studies also showed that ligation of PD1 with PDL1 can affect the activities of NK cells, TAMs and DCs as well [4–11]. In this regard, monoclonal antibodies (mAb) that block PD1/PDL1 interaction by targeting either PD1 or PDL1 have been shown to restore immune responses in tumor microenvironment, resulting in significant and sometimes, long-lasting anti-tumor activity in clinics for several cancers, including melanoma, lymphoma, non-small cell lung cancer, gastric and liver cancers [12].

EGFR/HER1 is a member of the epidermal growth factor receptor (EGFR) family and plays important roles in development and tumorigenesis, e.g. lung tumors [13,14]. HER receptors are often overexpressed or mutated in many tumors and thus are considered as important targets for anti-tumor therapy. Activation of HER receptors involves the homo- and hetero-dimerization of the extracellular domain of HER receptors (EGFR, HER2, HER3 or HER4) following ligand binding [15,16]. This leads to the formation of an asymmetric dimer of the intracellular tyrosine kinase domains (TKDs), which results in the allosteric activation and trans-phosphorylation of tyrosines in the tail of the TKDs [17]. EGFR stimulation can activate multiple intracellular signaling pathways, including PLC-γ-PKC, Ras-Raf-MEK, PI3K-Akt-mTOR and JAK2-STAT3 and thus play critical roles in tumor growth and metastasis [18–21]. To date, a number of anti-EGFR mAbs and receptor tyrosine kinase inhibitors have been approved for treatment of multiple cancers, including colorectal, head & neck, and non-small cell lung cancers [22–26].

* Corresponding authors.
E-mail addresses: zhuzhenping@3sbio.com (Z. Zhu), huanghaomin@3s-guojian.com (H. Huang).
[1] These authors contributed equally to this study.

Several approaches have been explored to further enhance the therapeutic efficacy of the anti-PD1/PDL1 and the anti-EGFR antibodies. Novel mAb to other immune checkpoint targets, for example antagonistic antibodies to LAG3, TIM3 and TIGIT, and agonistic antibodies to CD40, OX40 and 4-1BB, are being identified and developed [27,28]. Anti-EGFR antibody-based bispecific antibodies (BsAb) and antibody-drug conjugates (ADC) are also being studied [29–31]. Recently, combination therapies of two or more tumor-targeting mAbs, for example, anti-HER2 mAbs, trastuzumab and pertuzumab, in breast cancer, or two or more immune checkpoint inhibitor mAbs, for instance, an anti-PD1 mAb (nivolumab) and an anti-CTLA4 mAb (ipilimumab) in melanoma and NSCLC, or others, such as an anti-vascular endothelial growth factor (VEGF) mAb (bevacizumab) and an anti-PDL1 mAb (atezolizumab) in liver cancer, have been shown to be more efficacious than single antibody agents in the clinic [32,33]. To this end, combination of an antibody targeting EGFR with an antibody targeting PD1, or alternatively, a BsAb that simultaneously targets both EGFR and PD1, may provide a novel and promising strategy to effectively treat cancers. Two antitumor BsAbs have been approved for clinical use up to date. Catumaxomab was approved by the European Medicines Agency (EMA) for the treatment of malignant ascites in 2009 and Blinatumomab approved for adult patients with relapsed or refractory B cell precursor acute lymphoblastic leukemia (ALL) by the United States Food and Drug Administration (FDA) in 2014. Overall, there are more than 110 BsAbs in development and over 50 BsAbs have been studied in clinical trials [34].

In this study, we constructed and produced a BsAb comprising of an anti-EGFR antibody IgG and a single chain Fv (scFv) from an anti-PD1 antibody. The BsAb retained its binding activity to both targets and was able to simultaneously engage EGFR on tumor cell surface and PD1 on T cells. In addition to its direct anti-tumor activity via EGFR inhibition, the BsAb mediates a strong ADCC activity and activates antitumor immunity through blockade of PD1/PDL1 interaction. Further, the BsAb exhibits a potent direct tumor cell killing activity in the presence of T cells by activating T cells and, at the same time, physically joining the T cells with tumor cells. Our anti-PD1 x anti-EGFR BsAb represents a novel strategy to enhance cancer treatment efficacy through both growth factor receptor blockade and tumor-targeted immune activation.

Materials and methods

Cell culture and proliferation assays

Cell lines used in this study were obtained from American Type Culture Collection (ATCC) unless otherwise noted. Cells were cultured in 37 °C incubator with 5% CO_2 using standard cell culture methods and reagents, A431 cells (ATCC Cat#CRL-1555, human epidermoid carcinoma), an EGFR-overexpressing epidermal cell line, were cultured in RPMI-1640 with 10% FBS, 1% L-glutamine and 1% penicillin/streptomycin; MC38 cells (Jennio biotech, mouse colon cancer cells) were cultured in DMEM with 10% FBS; SW48 cells (ATCC Cat#CCL-231, human colorectal adenocarcinoma) were cultured in L-15 supplemented with 10% FBS; Peripheral blood mononuclear cells (PBMCs) from healthy donors (Saily Bio, Cat#SLB-HP) and T cells (Saily Bio, Cat#SLB-CD3T-10AN) were cultured in RPMI 1640 complete medium. HEK293E was cultured in freestyle 293 medium (Life technologies) with 1% Penicillin-Streptomycin. PD1-overexpressing Jurkat T cells (Promega, Cat#J1250) were cultured in RPMI-1640 with 10% FBS, 1% Sodium Pyruvate, 1% penicillin/streptomycin, 500 ug/ml G418, 1% MEM Non-Essential Amino Acids, 200 ug/ml Hygromycin B. Cell proliferation assays were conducted in 96-well plates with a starting confluence of 10-20% for 6 days. Cell viability was assessed using Cell Counting Kit-8 (Dojindo, Cat# CK04) according to manufactory's instruction.

Protein expression and purification

Constructs expressing the anti-PD1 x EGFR BsAb variants were generated using pTT5 vector (NRC Biotechnology Research Institute). The resulting expression vectors were transiently transfected into HEK293E cells using 1 ug/mL 25-kDa linear PEI (Polysciences, Inc.). 1 day after transfection, valproic acid (Sigma) was added to cell culture at a final concentration of 3 mM. On day 2 post-transfection, cells fed with medium comprising 10% GlutaMAX, 10% 400 g/L glucose and 80% freestyle 293 medium was added to the cell culture at 10% of the total volume. Conditioned medium was collected 5–6 days after transient transfection. BsAbs in the culture media were purified by MabSelect SuRe (GE) affinity columns using an Akta Avant 25 FPLC purification system. After equilibrating the column with buffer A (25mM sodium phosphate, 150 mM sodium chloride, pH=7.0), the culture media containing BsAbs were applied to the column, which was then eluted with buffer B (100 mM sodium citrate, pH=3.5) to collect the desired proteins. The eluted BsAbs were further polished by gel filtration on a SuperdexTM 200 column (GE) if necessary.

Indirect ELISA binding assay

96-well plates (Costar, Cat#9018) were coated with 1 μg/ml His-tagged EGFR-ECD or PD1 proteins (in-house) or other related proteins at 4 °C overnight. The plates were washed with phosphate-buffered saline (PBS) containing 0.05% Tween-20 (PBS-T), blocked for 1 h with PBS containing 2% bovine serum albumin (BSA) and incubated with serial dilutions of purified antibodies for 1 h at room temperature. The plates were washed with PBS-T for three times and incubated with Anti-Human IgG (Fc specific)−peroxidase antibody (Sigma, Cat#A0170) for 1 h at room temperature. The plates were washed and the reaction developed with TMB substrates. The plates were then read on a SpectraMax 190 reader (Molecular Devices) at 450 nm.

Flow cytometry on A431 cells

To measure anti-PD1 x EGFR BsAb binding affinity for EGFR-overexpressing cells, A431 cells (3×10^5) were incubated with 3-fold serial dilutions of the BsAb ranging from 500 nM to 0.23 nM in 200 μL serum-free RPMI 1640 at 4 °C for 1 h. Cells were washed three times with PBS and the bound antibody was incubated with FITC-conjugated Anti-Human IgG antibody (Sigma, Cat#F9512-2mL) at 4 °C for 30 min. Cells were washed and resuspended in 200 μL PBS and were analyzed on FACS (BECKMAN, Cytoflex).

ADCC assays

A431 tumor cells were grown in 96-well flat bottom plates at a density of 1×10^4 cells/50 uL/well in RPMI 1640 supplemented with 5% FBS. NK cells (ATCC, Cat#pta-8837) were grown in MEM with 0.2 mM Inositol, 2 mM L-glutamine, 12.5% FBS, 12.5% HS, 0.02mM folic acid, 0.1mM β-Mercaptoethanol and supplemented with 200 U/ml IL-2 at a density between 2×10^5cells/ml – 5×10^5 cells/ml. Serial dilutions of anti-PD1xEGFR BsAbs and control antibodies were added to each well in the presence of 5×10^4 NK cells/well for a final reaction volume of 150uL, and the plates were incubated for 3 h at 37°C and 5% CO_2. 3 h later, 50 μL LDH substrate was added into each well and incubated at room temperature for 15 min. The plates were then read at 490 nm on a SpectraMax 190 reader (Molecular Devices). The lysis % was converted from OD values according to the following formula: (OD_{sample}-OD_T-OD_{nk}) / OD_{lysis}*100%. The EC_{50} was calculated using GraphPad Prism 6 software (GraphPad Software). In the case of T cells, anti-CD28 antibody pre-activated T cells were used instead of tumor cells.

Tumor cell killing and cytokine release assays

Prior to use, SW48 cells were harvested in logarithmic phase and diluted to 1×10^5 cells/ml in RPMI 1640 supplemented with 5% FBS. 100uL SW48 cells were then added into the wells of 96-well flat bottom plates and incubated overnight at 37° C and 5% CO_2. Next day, 100 nM of various antibodies and controls were added to each well in the presence of 1×10^5 PBMC/50 uL/well for a final reaction volume of 150 uL, and the plates were incubated for 7 days at 37°C and 5% CO_2. 7 days later, 50 uL Cell-Titer Glo reagent (Promega, Cat#G7570) was added to each well and the plates incubated at room temperature for 5–10 min. The plates were then read on a MD SpectraMax i3 for luminescence at 500 ms. For cytokine release assays, 150uL supernatants were collected from each sample well 3 days after incubation at 37 °C and 5% CO_2. Cytokines in the supernatants were detected using Cytometric Bead Array (CBA) Human Th1/Th2 Cytokine kit II (BD, Cat#551809).

FACS to determine the bridging of T cells with tumor cells by the BsAb

Prior to use, PD1-overexpressing Jurkat T cells were stimulated by 1 μg/ml anti-CD3 mAb for 48h for enhanced PD1 expression. The pre-activated T cells were then labeled with Alexa Fluor 647-conjugated anti-PD1 mAb (Sinobiological, #MM18, with different epitopes from 609A) in the presence of anti-PD1 x EGFR BsAb (namely, T1), 609A (T2) and the BsAb plus 609A (T3) for 1h at room temperature respectively. In parallel, A431 tumor cells were harvested in logarithmic phase and labelled with Alexa-fluor 546-conjugated anti-EGFR mAb, HuML66 (patent no. #US9238690B2) produced in-house, with epitopes different from cetuximab) in the absence (namely, A1) or presence (A2) of cetuximab for 1h at room temperature. After 1h, the 647-Labeled T cells and 546-labeled A431 tumor cells were separately washed by PBS 3 times to remove antibodies, and then co-cultured together for 30min at room temperature at a ratio of 2:1 (T cells vs Tumor cells) as the following format T1+A1, T2+A2 and T3+A1, respectively. Samples were then subject to FACS (BECKMAN, Cytoflex) at a cell flow rate of 500–10,000 cells/sec. to analyze the ratio of conjugates of T cells with tumor cells.

Immunofluorescence microscopy

Prior to use, PD1-overexpressing Jurkat T cells (Promega) were stimulated by 1 μg/ml anti-CD3 mAb for 48 h for enhanced PD1 expression. The activated T cells were labeled with 200nM Alexa Fluor 488 (488)-conjugated anti-PD1 x EGFR BsAb (namely T1) or 488-conjugated anti-PD1 mAb (609A) (T2) for 1h at room temperature respectively. A431 tumor cells were labeled with 100 nM Alexa Fluor 546 (546)-conjugated anti-EGFR mAb (HuML66) in the presence (namely A1) or absence (A2) of cetuximab for 1h at room temperature respectively. 488-Labeled T cells were then co-cultured with 546-labeled A431 cells as the following formats T1+A2 or T2+A1 in PBS for 30min at room temperature followed by transferring into 6-well plates pre-coated with poly-lysine prior to fixation by 4% paraformaldehyde. Images of conjugated T and tumor cells by the BsAb were visualized with an LCAch N 40x/0.55 PhP objective (IX53, Olympus).

Xenografted and syngeneic tumor models

Animal care and in vivo experiments were approved (The approval Code for SW48 xenograft model: AS-2018-052; for MC38 syngeneic model: AS-2018-038) by institutional IACUC of Sunshine Guojian Pharmaceutical (Shanghai) Co. Ltd and performed under protocols. SW48 cell line-derived xenograft models were established in 6-week female Balb/c nude mice (purchased from Charles River Laboratories) by subcutaneous injection of 3×10^6 SW48 mixed with 50% matrigel. When tumors had reached a size of about 150 mm^3, the animals were divided into groups with comparable tumor sizes and treated as described in the text and figures, i.p. twice a week. Human PDL1-transfected MC38

cell line-derived syngeneic models were established in 18–20 female C57BJ/6J-PDCD1em1(Hpdcd1)/Smoc mice (purchased from Shanghai Model Organisms) by subcutaneous injection of 1×10^6 cells. C57BJ/6J-PDCD1em1 (Hpdcd1)/Smoc mice are transduced with human PDCD1 gene and express human PD-1 protein. When tumors had reached a size of about 150 mm^3, the animals were divided into groups with comparable tumor sizes and treated as described in the text and figures, i.p. twice a week. Human IgG was used as the negative control. Tumor growth was measured per 3–4 days and calculated using the formula $V = LW^2/2$ (where V= volume, L=length and W =width).

Statistical analysis

All numerical data were presented as mean $\pm$ standard deviation (SD) except for mouse xenograft data which were presented as mean $\pm$ standard error (SE). Numerical data processing and statistical analysis were performed with Microsoft Excel and GraphPad Prism 6 software. P values were calculated using unpaired two-tailed Student-t test. In all tests, differences with P values < 0.05 ($*$) were considered to be statistically significant.

Results

Construction and production of the anti-PD1 x EGFR BsAb

To construct the BsAb, we fused the scFv of an anti-PD1 mAb (SSGJ-609A or 609A) to the IgG scaffold of the anti-EGFR antibody, cetuximab (Erbitux), a FDA-approved antibody for the treatment of colorectal cancer and head and neck cancer [33]. We first examined the effect of the scFv/IgG orientation in the BsAb molecule on its target binding activity by fusing the scFv to either the N-terminus or the C-terminus of the IgG heavy chain. Results showed that the anti-PD1 (609A) scFv fused to the N-terminus exhibited 10-fold better binding affinity for PD1-overexpressing CHO cells than that fused to the C-terminus (Fig. S1). Thus, the BsAb with anti-PD1 scFv attached to the N-terminus of cetuximab, namely anti-PD1 x EGFR BsAb, was selected for further characterization (Fig. 1A). The BsAb was expressed in mammalian cell culture and purified by a single-step Protein A chromatography (Fig. 1B). The BsAb also showed a good thermostability with a Tm1/Tm2/Tm3 of over 61 °C, 71°C and 83 °C respectively (Fig. 1C).

The anti-PD1 x EGFR BsAb retained full binding activities of the parental mAb

The anti-PD1 x EGFR BsAb dose-dependently bound to PD1 and EGFR in ELISA assays. The EC$_{50}$ (the antibody concentration required for 50% of maximum binding) of the BsAb for EGFR is 1.27 nM, which is comparable to that of cetuximab (1.09 nM) (Fig. 2A). The EC$_{50}$ of the BsAb for human PD1 is 0.19 nM, compared to that of 0.15 nM of the parental anti-PD1 mAb, 609A (Fig. 2B).

Next we tested the ability of the BsAb to bind to the receptors on cell surface using FACS. The EC$_{50}$ of the BsAb binding to A431 cells, a human epidermoid cancer cell line that overexpresses EGFR, is 4.38nM, which is comparable to that of cetuximab, whose EC$_{50}$ is 4.98 nM (Fig. 2C). The EC$_{50}$ of the BsAb for PD1-overexpressing CHO cells is 1.53 nM, compared to that of 1.62 nM of 609A (Fig. 2D).

A bridging ELISA was utilized to confirm that the BsAb is capable of simultaneously binding to its two targets. As shown in Fig. 2E, the BsAb was able to cross-link the two targets, EGFR and PD1, whereas the mono-specific antibodies, 609A and cetuximab, failed to do so (Fig. 2E).

The anti-PD1 x EGFR BsAb retained full biological activities of the parental antibody in cell-based assays

In an in-vitro tumor cell growth assay, the BsAb inhibited the proliferation of EGFR-overexpressing A431 cells at an IC$_{50}$ (the antibody
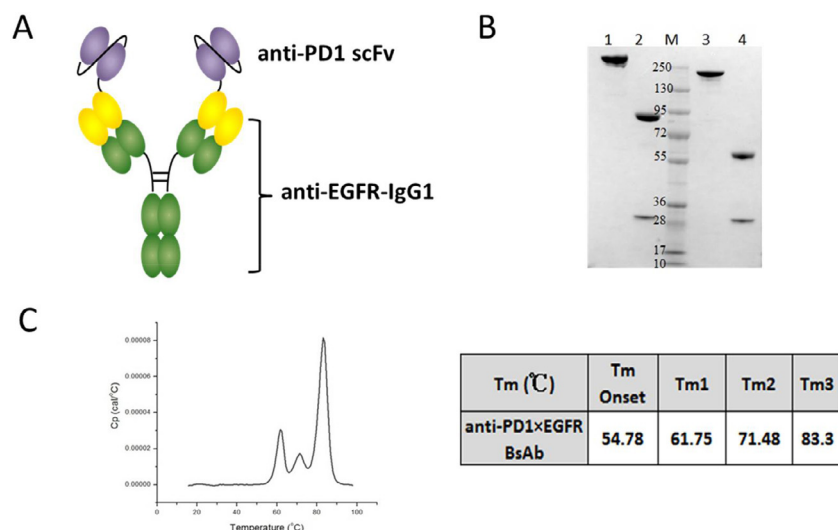
Fig. 1. The structure and properties of the anti-PD1 x EGFR BsAb. A) Schematics of the anti-PD1 x EGFR BsAb structure. B) SDS-PAGE showed non-reduced and reduced anti-PD1 x EGFR BsAb. Lane1: Non-reduced BsAb; Lane2: reduced BsAb; Lane3: Non-reduced cetuximab; Lane4: reduced cetuximab; M: Molecular weight marker. C) Differential scanning calorimetry (DSC) of anti-PD1xEGFR BsAb shows T_{onset}=54.8 °C and $T_m 1/2/3$=61.8 °C/ 71.5°C/ 83.3 °C.

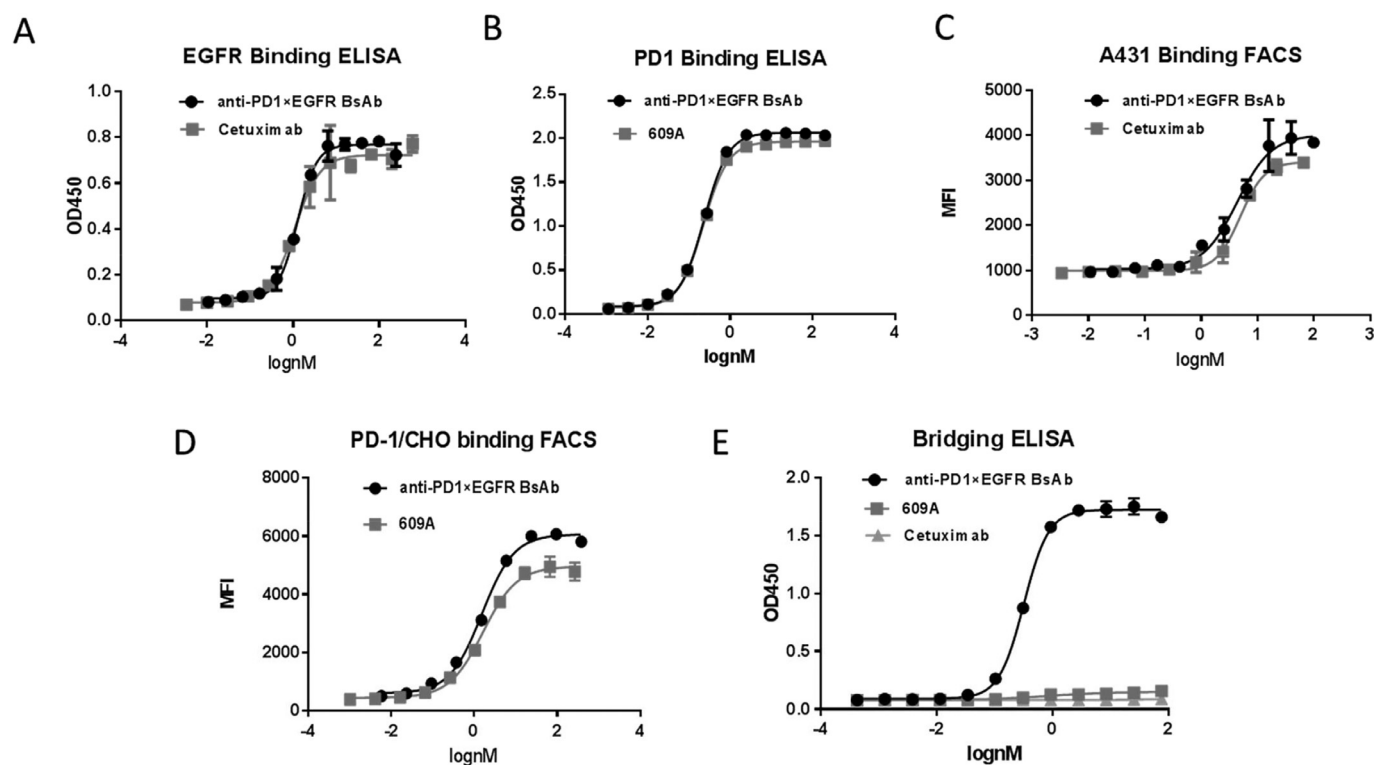| Tm (℃)	Tm Onset	Tm1	Tm2	Tm3
anti-PD1×EGFR BsAb	54.78	61.75	71.48	83.3

Fig. 2. Anti-PD1 x EGFR BsAb simultaneously bound to PD-1 and EGFR. A) The binding affinity of the BsAb for EGFR was measured by ELISA. Cetuximab was used as the positive control. B) The binding affinity of the BsAb for PD1 was measured by ELISA and compared to that of the parental anti-PD1 mAb, 609A. C) The ability of the BsAb to bind to A431, an EGFR-overexpressing cancer cell line, was measured by FACS and compared to that of cetuximab. D) The ability of the BsAb to bind to PD1-overexpressing CHO cells was measured by FACS and compared to that of the parental anti-PD1 mAb, 609A. E) A bridging ELISA was setup in a way that EGFR proteins were coated on the plates followed by addition of indicated antibodies and biotin-labelled PD1 proteins sequentially. Strepavidin-HRP was added to visualize the positive binders. Result confirms that the BsAb is capable of simultaneously cross-linking its two targets, EGFR and PD1.

concentration that inhibits 50% of cell proliferation) of 0.81 nM, which is similar to that of cetuximab at 0.93 nM (Fig. 3A). In a PD1/PDL1 blockade cell-based assay (Promega, Cat#J1250), the BsAb blocked PD1/PDL1 cell signaling with an IC_{50} of 1.43nM, compared to that of 0.89 nM for the parental anti-PD1 antibody, 609A (Fig. 3B). These results confirmed that the BsAb retained its dual-functionality to directly inhibit tumor cell growth and to block PD1-mediated negative cellular signaling in T cells.

The anti-PD1 x EGFR BsAb showed potent ADCC towards EGFR-overexpressing tumor cells but not T cells

It is known that antibody dependent cellular cytotoxicity (ADCC) is one of the mechanisms of action for cetuximab. Here we examined the ADCC of the BsAb towards cancer cells as well as T cells. As expected, the BsAb exhibited strong ADCC towards A431 cancer cells with potency comparable to that of cetuximab (Fig. 4A). Intriguingly, the BsAb
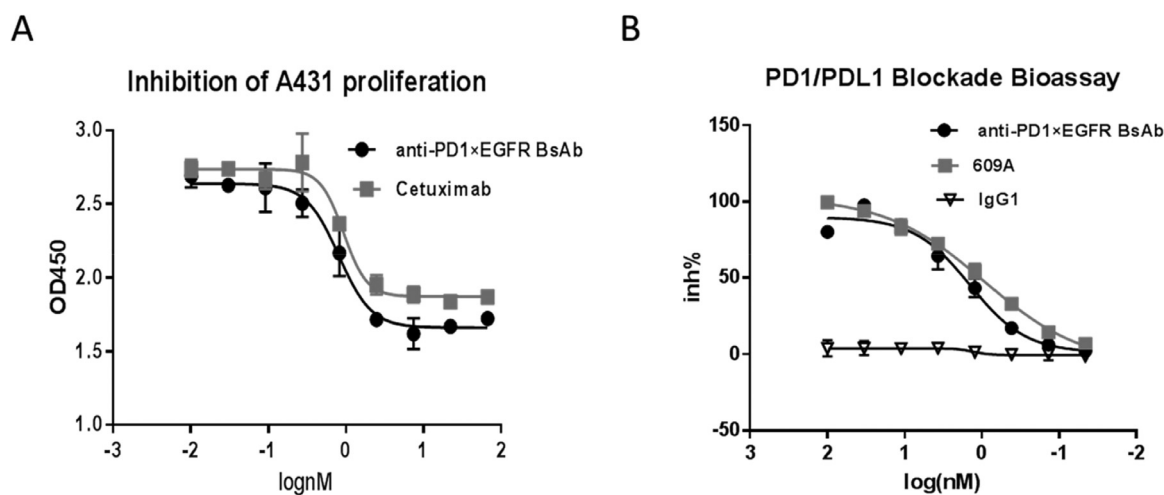
Fig. 3. Anti-PD1 x EGFR BsAb inhibited proliferation of EGFR-overexpressing tumor cells and blocked PD1/PDL1 interaction in cell-based bioassays. A) The BsAb inhibited proliferation of EGFR-overexpressing A431 cancer cells in a dose-dependent manner similar to cetuximab. B) The ability of the BsAb to block the PD1/PDL1 signaling was measured and compared to that of the parental anti-PD1 mAb, 609A, using a PD1/PDL1 blockade cell-based assay (Promega) according to the manufacture's instruction. A non-specific IgG1 was used as the negative control.
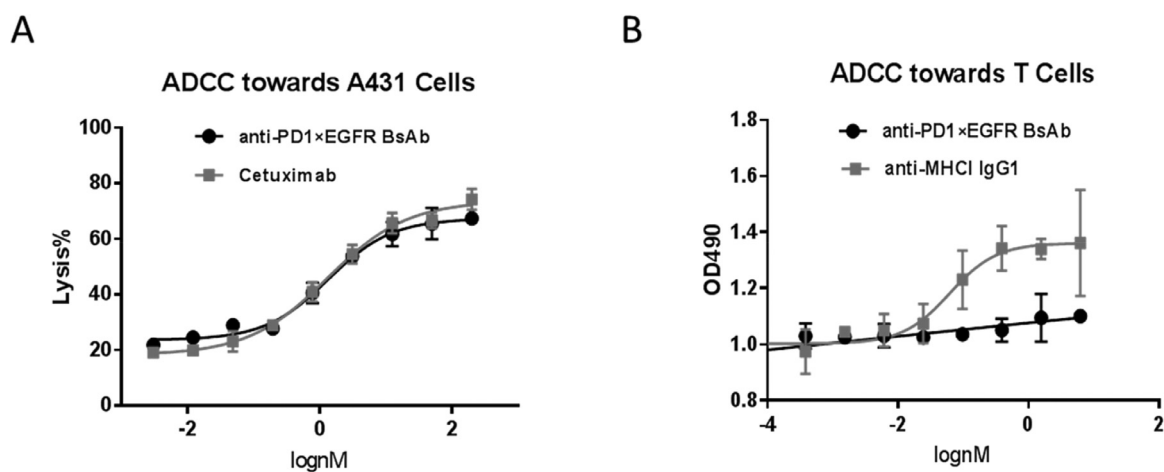

Fig. 4. Anti-PD1 x EGFR BsAb retained ADCC towards tumor cells but not T cells. A) The BsAb exhibited similar potency in lysing tumor cells to that of cetuximab in the ADCC assay. B) The BsAb failed to mediate significant ADCC towards T cells, whereas an anti-MHC1 IgG1 antibody showed strong potency in lysing T cells in a dose-dependent manner.

did not show measurable ADCC towards T cells, whereas a positive control antibody targeting the MHC-I molecule of T cells exhibited a strong cytotoxicity effect (Fig. 4B). Taken together, these results suggest that the 609A scFv in the BsAb format is not efficient at triggering a meaningful ADCC activity towards T cells when fused to the N-terminus of an IgG heavy chain, perhaps due to an undesirable tertiary relationship (or spacing) between the binding of PD1 on T cell (the target) surface and the FcγR engagement on the effector cells.

The anti-PD1 x EGFR BsAb is capable of engaging cytotoxic T cells for direct tumor cell killing

Next we tested whether the BsAb is capable of inducing direct tumor cell killing by engaging tumor cells and T cells simultaneously. In this experiment, we cultured SW-48, a colorectal cancer cell line that expresses both EGFR and PD-L1 (data not shown), with human PBMCs in the presence of various antibodies. Cetuximab significantly reduced the number of live tumor cells whereas the anti-PD1 mAb, 609A, only exhibited a moderate inhibitory activity. Combination of cetuximab and 609A did not further enhance the antitumor effect of cetuximab. Intriguingly, anti-PD1 x EGFR BsAb demonstrated a significant more potent tumor

inhibition compared to that of cetuximab alone or in combination with 609A (Fig. 5A).

FACS analysis revealed that, in the presence of the BsAb, but not the simple combination of the two parent mAb, there is formation of conjugates of tumor cells and T cells (Fig. 5B, upper right corner in the left and middle panels). The conjugation could be blocked by the monospecific anti-PD1 antibody, 609A (Fig. 5B, right panel), suggesting that the BsAb is capable of directly cross-linking the two cell populations via simultaneous binding to its targets on both tumor and T cells. This is further confirmed by immunofluorescence microscopy. Incubation of the tumor cells with T cells in the presence of the BsAb led to the formation of "rosettes" where the tumor cells were surrounded by one or more T cells, in some cases, a single T cell was seen in contact with several tumor cells (Fig. 5C). No significant tumor-T cells interaction was observed when the two cell population was incubated with a mixture of cetuximab and 609A (Fig. 5C).

IFN-γ has long been implicated as a hallmark of Th1-polarized antitumor immunity [36]. Next, we analyzed IFN-γ production over the course of incubation of SW-48 cancer cells with the BsAb in the presence of human PBMC. The BsAb induced a much more significant IFN-γ production, which was peaked on day 3 post antibody treatment, and
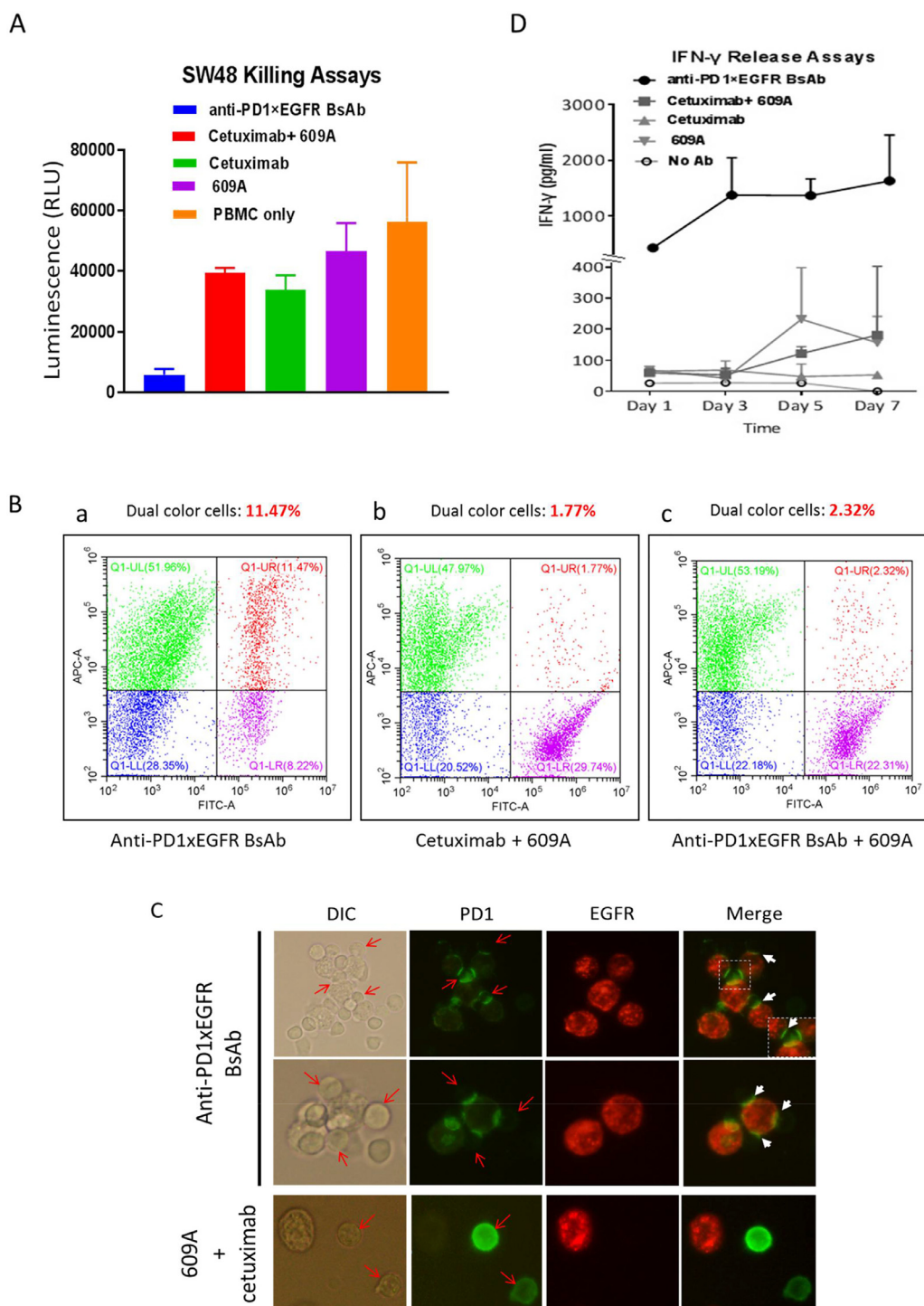
Fig. 5. Anti-PD1 x EGFR BsAb is capable of engaging cytotoxic T cells for direct tumor cell killing. A) Human PBMCs were mixed with SW48 tumor cells in the presence of 100 nM indicated antibodies. The number of live cells was measured as Relative Luminescence Units (RLU). PBMC only: tumor cells mixed with PBMC in the absence of antibodies. Cetuximab+609A: combination of cetuximab with the anti-PD1 mAb, 609A. B) PD1-overexpressing Jurkat T cells (Promega) pre-labeled with Alexa Fluor 647-conjugated anti-PD1 mAb (Sinobiological, #MM18) were mixed with A431 cells pre-labelled with Alexa fluor 546-conjugated anti-EGFR mAb (HuML66) in the presence of a) the BsAb, b) the mixture of cetuximab and 609A, c) the BsAb plus 609A, respectively. The group in red (pseudo-color) (upper right corner) are cells that have dual emission signals (MFI $>1 \times 10^5$ for FITC-A and MFI $>3 \times 10^3$ for APC-A), meaning that both cells were associated together; The group in green (pseudo-color) (upper left corner) are T cells labeled with Alexa Fluor 647-conjugated anti-PD1 mAb (MFI$>3 \times 10^3$ for APC-A); The group in purple (pseudo-color) (lower right corner) are A431 cells labeled with Alexa fluor 546-conjugated anti-EGFR mAb (MFI$>1 \times 10^5$ for FITC-A). C) Immunofluorescence microscopy showing co-staining of PD1 (green) on T cells and EGFR (red) on A431 tumor cells for samples treated with the BsAb or a mixture of the anti-PD1 mAb (609A) plus cetuximab. Note the formation of "rosettes" where tumor cells are surrounded by multiple T cells, and in other cases, a single T cell is in contact with several tumor cells (the inset), in the presence of the BsAb. The mixture of 609A and cetuximab failed to induce the formation of "rosettes". Red arrows denote T cells (DIC channel) which were barely seen for PD1 staining (green channel) owing to the rearrangement of PD1. White arrowheads denote the synapses formed by PD1 rearrangement. D) Human PBMCs were mixed with SW48 tumor cells in the presence of 100nM indicated antibodies. The concentrations of IFNγ secreted into the medium were measured and plotted against the days of treatment. No Ab: tumor cells mixed with PBMCs in the absence of any antibodies.
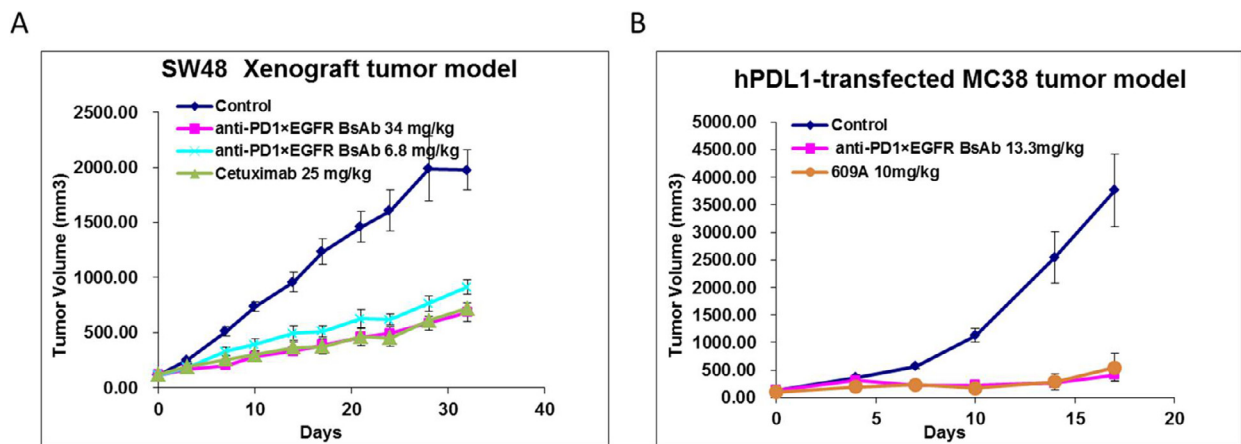
Fig. 6. Anti-PD1 x EGFR BsAb exhibited potent antitumor effects in vivo. A) A vehicle control (diamond), the BsAb (square & cross) and cetuximab (triangle) were i.p. injected into mice bearing SW48 tumor at the indicated doses. Tumor volumes (mm^3) were measured at the indicated time points. B) A vehicle control (diamond), the BsAb (square) and anti-PD1 mAb (solid circle) were i.p. injected into mice bearing human PDL1-transfected MC38 tumor at the indicated doses. Tumor volumes (mm^3) were measured at the indicated time points.

maintained at the high level through the end of the experiment on day 7, compared to cetuximab, 609A or the combination of the two (Fig. 5D). The increase of IFN-γ mediated by the BsAb could not be attributed to proliferation of PBMC, as the number of CD8+ T cells remained mostly unchanged throughout the course of experiments for all groups (data not shown).

The anti-PD1 x EGFR BsAb is potent in inhibition of tumor growth in both xenografted and syngeneic tumor models

We next evaluated the antitumor effects of each of the two arms of the BsAb in vivo. We used an SW48 xenograft model to measure the efficacy of the BsAb for EGFR blockade. In this study, cetuximab suppressed 70% of SW48 tumor growth at the dose of 25 mg/kg on day 32 post treatment. The BsAb was equally potent in suppressing the tumor growth, in a dose dependent manner, with inhibition rates of 60% and 70% at 6.8 mg/kg and 34 mg/kg (which is the equal molar dose of 25 mg/kg cetuximab) respectively (Fig. 6A).

Using a human PDL1-transfected MC38 tumor cell line in a human PD1 transgenic syngeneic mouse model, we analyzed the antitumor activities of the anti-PD1 arm of the BsAb. In line with our previous studies, anti-PD1 mAb, 609A, effectively inhibited around 90% of tumor growth at a dose of 10 mg/kg on day 21. Similarly, the BsAb also inhibited around 90% of tumor growth at an equal molar dose of 13mg/kg (Fig. 6B). Taken together, these results indicated that each arm of anti-PD1 x EGFR BsAb retained the antitumor efficacy to the level comparable to their parental mAb in vivo. Due to the fact that both the functional domains (anti-PD1 and anti-EGFR) of the BsAb do not have cross-reactivity with their mouse counterparts, we were unable to simultaneously assess the dual antitumor efficacy of the BsAb in one single animal model, thus addressing the potential synergistic antitumor effect of the BsAb in these mouse models.

Discussion

Both tumor-targeted therapies via specific mAb directed against tumor-associated antigens, e.g., EGFR and HER2 and tumor immune therapies via checkpoint inhibitor blockade, e.g., anti-PD1/PDL1 mAb, have demonstrated significant and meaningful clinical benefits in multiple cancers [26,32,33,35,37]. The effectiveness of these therapies, however, remains modest and many patients are either refractory or become resistant to the treatment over times. Many efforts are being attempted to develop more efficacious approaches, for example, by identifying new targets and/or exploring various combination therapies of

different classes of antitumor agents. It is well known that tumors are highly heterogeneous, comprising of not only the tumor cells but multiple other tissues and cells including neo-vasculature (proliferating endothelial cells), fibroblasts, and various immune cells such as T cells, macrophages and other mononuclear cells. Co-targeting different components in a tumor thus represents a rational and promising approach to enhance the overall therapeutic efficacy and to address the issue of tumor resistance to the existing therapies.

In this study, we devised a strategy to combine conventional targeted therapy with immune checkpoint blockade (anti-PD1/PDL1) by a BsAb approach to treat solid tumors. In the BsAb embodiment, the anti-PD1 antibody is directed to the tumor microenvironment by a second antibody targeting a tumor associated antigens expressed in the tumors [29]. The BsAb, anti-PD1 x EGFR BsAb, was constructed by fusion of two anti-PD1 scFv symmetrically to the N-terminus of the heavy chains of cetuximab. The orientation of the anti-EGFR IgG and the anti-PD1 scFvs is important, as swapping the anti-PD1 scFvs from the N to the C-terminus of cetuximab IgG heavy chains significantly (by 10-fold) reduced the binding of the BsAb to PD1-overexpressed CHO cell surface. This observation suggests that the position of 609A scFv in the BsAb molecule may affect its overall folding/structure (thus reducing its binding activity), and/or influence its access to the binding epitopes on PD1 on the cell surface.

There are in theory several rationales for co-targeting EGFR on tumor cells and PD1 on T cells via a BsAb: 1) accumulating evidence demonstrated that stimulation of EGFR signaling can suppress immune responses and enhance the tumor cell evasion of immune surveillance, including induction of PDL-1 overexpression on the surface of tumor cells, stimulation of VEGF, IL6, IL10 secretion, activation of regulatory T cells (Tregs) and downregulation of T cell chemokines [38–45]. Inhibition of EGFR signaling in tumor cells, therefore, not only can exert direct antitumor activity but also may create a more favorable anti-tumor immune microenvironment [40,46]; 2) By targeting EGFR-overexpressing tumor cells, anti-PD1 x EGFR BsAb may enhance the antibody localization to specifically target and activate T cells and other immune cells within the tumor microenvironment [29]; 3) the BsAb simultaneously targeting EGFR on tumor cell surface and PD1 on T cells may likely be able to create direct cell-cell interaction/engagement of the tumor cells and the immune cells, and leads to the formation of immunological synapse, resulting in CD8$^+$ T cell activation and potent tumor cell killing [30,47].

As expected, the BsAb retained the biological activities of each of its parent mAb. The BsAb efficiently bound to EGFR and PD1, both independently and simultaneously (Fig. 2). Further, the BsAb was as effec-
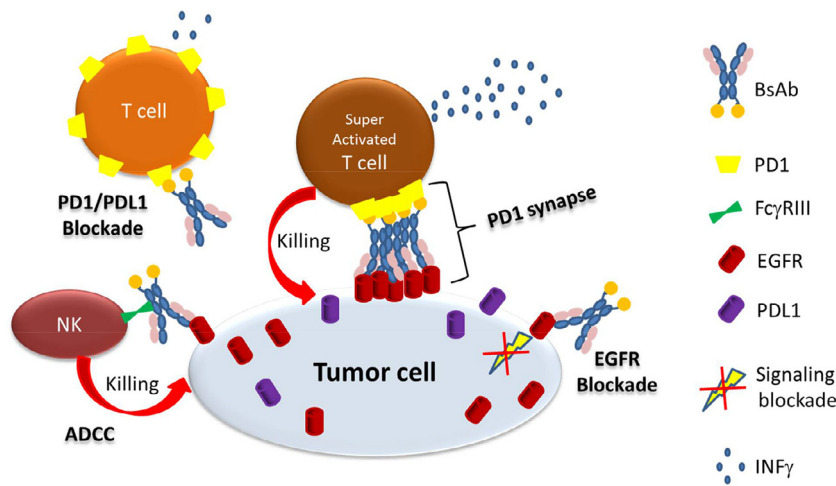
Fig. 7. Schematic of the mechanisms of Anti-PD1 x EGFR BsAb mediated tumor cell killing. Multiple ways might be employed by the BsAb to kill tumor cells, including PD1 synapse formation which leads to super activation of T cells, resulting in increased IFNγ secretion, T cell activation induced by PD1/PDL1 blockade, EGFR mediated growth signaling blockade, and ADCC induced by the BsAb binding to EGFR.

tive as the parental mAb in inhibiting proliferation of EGFR-expressing tumor cells and in activating T cells via blocking PD1/PDL1 interaction (Fig. 3). In animal studies, the BsAb demonstrated equal potency to cetuximab in a nude mouse xenografted tumor model (a system without human T cell presence), and to the anti-PD1 mAb (SSGJ-609A) in the human PD1-transgenic mouse syngeneic tumor model (where the tumor cells does not express human EGFR) (Fig. 6). It is unfortunate that there are no appropriate animal models available to date where the antitumor activity of the anti-EGFR and the anti-PD1 mAb, or the BsAb, could be examined simultaneously within a single system, as both the parental mAb only specifically recognize human targets but not their mouse counterparts.

In this study, we showed that the BsAb, with an IgG1 scaffold, is potent in mediating ADCC towards the EGFR-expressing tumor cells but not to PD1-expressing T cells. It is generally acknowledged that ADCC mediated by mononuclear cells (in particular NK cells) is one of the mechanisms of action for cetuximab, an IgG1 subtype, to kill tumors [48]. On the other hand, IgG4, which is much less potent in FcγRIII binding and mediating ADCC, has been the universal choice when constructing anti-PD1 antibodies, to alleviate the concerns over innocent (or bystander) T cell killing by the ADCC activity. Here, we constructed the BsAb using cetuximab IgG1 as the scaffold. As expected, the BsAb retained strong ADCC when compared to cetuximab. Interestingly, the BsAb did not show significant ADCC activity towards T cells. Since the anti-PD1 scFv was fused to the N-terminus of the heavy chain of an IgG1 scaffold, this observation suggests that in this case, perhaps, the physical distance (or spacing) between the target antigen binding (at the far end of the N-terminus) and the FcγR interaction by the BsAb may not be ideal in mediating an efficient ADCC towards the target cells. This result indicates that it is feasible to construct an IgG1-like (Fc-containing) BsAb that retains ADCC towards one target cell while sparing the other, via rational molecular design.

The BsAb was much more efficacious at inhibiting tumor cell growth in the presence of PBMC, compared to cetuximab, alone or in combination with the anti-PD1 antibody. This enhanced antitumor activity by the BsAb could not be entirely attributed to PD1/PDL1 blockade as addition of the anti-PD1 mAb to cetuximab failed to show any synergy. Staining of T cells and tumor cells (A431) confirmed the association of T cells with tumor cells by the bispecific antibody, whereas combining of monoclonal antibodies failed to do so (Fig. 5B and C). These data implied that physical ligation of tumor cells with T cells by the PD1-based bispecific antibodies might increase T cell-mediated immune responses which could not be achieved by simply mixing the two monoclonal antibodies together. It was shown that engagement of target cells with T cells could facilitate formation of immunological synapses which play important roles in T cell-mediated cytotoxicity [47]. It is plausible that

the BsAb also induced synapse formation. Li and colleagues showed that the distance between the tumor cell membrane and the binding epitopes of bispecific antibodies was critical for the formation of synapses – a shorter distance would facilitate more efficient T cell synapse formation [47]. Intriguingly, Cetuximab binds to the domain III proximal to the domain IV of EGFR ECD [49], suggesting that the proximity of binding epitopes of the bispecific antibody to the cell membrane might facilitate the formation of synapses when ligating the tumor cells and T cells. Yet, we cannot rule out the other possibilities that the BsAb could enhance T cell-mediated cell killing via other mechanisms. Indeed, we showed that the BsAb induced a much higher level IFN-γ production when co-incubated with tumor cells and PBMC, compared to cetuximab, the anti-PD1 mAb or the combination of the two (Fig. 5D). Thus, the BsAb may not only serve as a cell engager, like those anti-TAA x anti-CD3 BsAbs, to cross-link T cells with tumor cells, but at the same time to activate T cells to be more efficient at killing tumor cells in its proximity (Fig. 7) [50].

In summary, here we engineered and produced a novel anti-PD1 x anti-EGFR BsAb and demonstrated the BsAb was more potent than the individual mAb and their combination at inhibiting tumor growth. Our data suggest that the BsAb may exert its potent antitumor activity via multiple mechanisms of action, including direct tumor growth inhibition, ADCC, T cell activation, T cell/tumor cell engagement and potent direct tumor cell killing. Taken together, our anti-PD1 x anti-EGFR BsAb represents a novel and potent antitumor agent that warrants further development in the treatment of multiple cancers.

Declaration of Competing Interest

The authors declare no potential conflicts of interest. All authors are employees of Sunshine Guojian Pharmaceutical (Shanghai) when the study was carried out.

CRediT authorship contribution statement

Li Li: Investigation, Methodology, Data curation, Formal analysis. **Lan Deng:** Data curation, Formal analysis, Investigation. **Xiaoqing Meng:** Data curation. **Changling Gu:** Validation. **Li Meng:** Data curation, Formal analysis. **Kai Li:** Data curation. **Xuesai Zhang:** Data curation, Writing - original draft. **Zhenping Zhu:** Conceptualization, Data curation, Supervision, Writing - review & editing. **Haomin Huang:** Conceptualization, Data curation, Supervision, Validation, Writing - original draft, Writing - review & editing.

Acknowledgments

Funding

Supplementary materials

Supplementary material associated with this article can be found, in the online version, at doi:10.1016/j.tranon.2020.100918.

Reference

[1] F.R. Balkwill, M. Capasso, T. Hagemann, The tumor microenvironment at a glance, J. Cell Sci. 125 (2012) 5591–5596, doi:10.1242/jcs.116392.

[2] G.M. Konjević, A.M. Vuletić, K.M. Mirjačić Martinović, A.K. Larsen, V.B Jurišić, The role of cytokines in the regulation of NK cells in the tumor environment, Cytokine 117 (2019) 30–40.

[3] H. Dong, S.E. Strome, D.R. Salomao, H. Tamura, F. Hirano, D.B. Flies, P.C. Roche, J. Lu, G. Zhu, K. Tamada, V.A. Lennon, E. Celis, L. Chen, Tumor-associated B7-H1 promotes T-cell apoptosis: a potential mechanism of immune evasion, Nat. Med. 8 (8) (2002) 793–800, doi:10.1038/nm730.

[4] F. Vari, D. Arpon, C. Keane, M.S. Hertzberg, D. Talaulikar, S. Jain, Q. Cui, E. Han, J. Tobin, R. Bird, D. Cross, A. Hernandez, C. Gould, S. Birch, M.K. Gandhi, Immune evasion via PD-1/PD-L1 on NK cells and monocyte/macrophages is more prominent in Hodgkin lymphoma than DLBCL, Blood 131 (16) (2018) 1809–1819, doi:10.1182/blood-2017-07-796342.

[5] X.L. Iraolagoitia, R.G. Spallanzani, N. Torres, R.E. Araya, A. Ziblat, C.I. Domaica, J.M. Sierra, S.Y. Nuñez, F. Secchiari, T.F. Gajewski, N.W. Zwirner, M.B. Fuertes, NK cells restrain spontaneous antitumor CD8+ T cell priming through PD-1/PD-L1 interactions with dendritic cells, J. Immunol. 197 (3) (2016) 953–961, doi:10.4049/jimmunol.1502291.

[6] M. Giuliani, B. Janji, G. Berchem, Activation of NK cells and disruption of PD-L1/PD-1 axis: two different ways for lenalidomide to block myeloma progression, Oncotarget 8 (14) (2017) 24031–24044, doi:10.18632/oncotarget.15234.

[7] G. Hartley, L. Chow, D.T. Ammons, W.H. Wheat, S.W. Dow, Programmed cell death ligand 1 (PD-L1) signaling regulates macrophage proliferation and activation, Cancer Immunol. Res. 6 (10) (2018) 1260–1273, doi:10.1158/2326-6066.CIR-17-0537.

[8] S. Su, J. Zhao, Y. Xing, X.Q. Zhang, J. Liu, Q. Ouyang, J. Chen, F. Su, Q. Liu, E. Song, Immune checkpoint inhibition overcomes ADCP-induced immunosuppression by macrophages, Cell 175 (2) (2018) 442–457, doi:10.1016/j.cell.2018.09.007.

[9] M. Versteven, J.M. Den Bergh, E. Marcq, E. Smits, V.V. Tendeloo, W. Hobo, E. Lion, Dendritic Cells, Programmed Death-1 Blockade, A joint venture to combat cancer, Front. Immunol. 9 (2018) 394, doi:10.3389/fimmu.2018.00394.

[10] J.A. Brown, D.M. Dorfman, F. Ma, E.L. Sullivan, O. Munoz, C.R. Wood, E.A. Greenfield, G.J. Freeman, Blockade of programmed death-1 ligands on dendritic cells enhances T cell activation and cytokine production, J. Immunol. 170 (3) (2003) 1257–1266, doi:10.4049/jimmunol.170.3.1257.

[11] D. Han, J. Liu, C. Chen, L.H. Dong, Y. Liu, R. Chang, X. Huang, Y. Liu, J. Wang, U. Dougherty, M.B. Bissonnette, B. Shen, R.R. Weichselbaum, M.M. Xu, C. He, Anti-tumour immunity controlled through mRNA m 6 A methylation and YTHDF1 in dendritic cells, Nature 566 (7743) (2019) 270–274, doi:10.1038/s41586-019-0916-x.

[12] M.F. Sanmamed, L. Chen, A paradigm shift in cancer immunotherapy: from enhancement to normalization, Cell 175 (2) (2018) 313–326, doi:10.1016/j.cell.2018.09.035.

[13] J. Schlessinger, Receptor tyrosine kinases: legacy of the first two decades, Cold Spring Harb. Perspect. Biol. 6 (3) (2014), doi:10.1101/cshperspect.a008912.

[14] V. Jurisic, V. Vukovic, J. Obradovic, L.F. Gulyaeva, N.E. Kushlinskii, N. Djordjević, EGFR Polymorphism and survival of NSCLC patients treated with TKIs: a systematic review and meta-analysis, J. Oncol. (2020) 1973241, doi:10.1155/2020/1973241.

[15] T. Kiuchi, E. Ortizzapater, J. Monypenny, D.R. Matthews, L.K. Nguyen, J. Barbeau, O. Coban, K. Lawler, B. Burford, D.J. Rolfe, E. de Rinaldis, D. Dafou, M.A. Simpson, N. Woodman, S. Pinder, C.E. Gillett, V. Devauges, S.P. Poland, G. Fruhwirth, P. Marra, Y.L. Boersma, A. Plückthun, W.J. Gullick, Y. Yarden, G. Santis, M. Winn, B.N. Kholodenko, M.L. Martin-Fernandez, P. Parker, A. Tutt, S.M. Ameer-Beg, T. Ng, The ErbB4 CYT2 variant protects EGFR from ligand-induced degradation to enhance cancer cell motility, Sci. Signal 7 (339) (2014) 1–14, doi:10.1126/scisignal.2005157.

[16] P. Littlefield, L. Liu, V. Mysore, Y.B. Shan, D.E. Shaw, N. Jura, Structural analysis of the EGFR/HER3 heterodimer reveals the molecular basis for activating HER3 mutations, Sci. Signal 7 (354) (2014), doi:10.1126/scisignal.2005786.

[17] M.A. Lemmon, J. Schlessinger, K.M. Ferguson, The EGFR family: not so prototypical receptor tyrosine kinases, Cold Spring Harb. Perspect. Biol. 6 (4) (2014), doi:10.1101/cshperspect.a020768.

[18] D. Anderson, C.A. Koch, L. Grey, C. Ellis, M.F. Moran, T. Pawson, Binding of SH2 domains of phospholipase C gamma 1, GAP, and Src to activated growth factor receptors, Science 250 (4983) (1990) 979–982, doi:10.1126/science.2173144.

[19] P.M. Navolanic, L.S. Steelman, J.A. Mccubrey, EGFR family signaling and its association with breast cancer development and resistance to chemotherapy (Review), Int. J. Oncol. 22 (2) (2003) 237–252, doi:10.3892/ijo.22.2.237.

[20] O.K. Park, T.S. Schaefer, D. Nathans, In vitro activation of Stat3 by epidermal growth factor receptor kinase, PNAS 93 (24) (1996) 13704–13708, doi:10.1073/pnas.93.24.13704.

[21] Y. Yarden, B. Shilo, SnapShot: EGFR signaling pathway, Cell 131 (5) (2007) 1018, doi:10.1016/j.cell.2007.11.013.

[22] P.M. Boland, W.W. Ma, Immunotherapy for colorectal cancer, Cancers 9 (5) (2017) 50, doi:10.3390/cancers9050050.

[23] C.S. Grasso, M. Giannakis, D.K. Wells, T. Hamada, X.M.J. Mu, M.J. Quist, J.A. Nowak, R. Nishihara, Z.R. Qian, K. Inamura, T. Morikawa, K. Nosho, G. Abril-Rodriguez, C. Connolly, H. Escuin-Ordinas, M.S. Geybels, W.M. Grady, L. Hsu, S. Hu-Lieskovan, J.R. Huyghe, Y.J. Kim, P. Krystofinski, M.D.M. Leiserson, D.J. Montoya, B.B. Nadel, M. Pellegrini, C.C. Pritchard, C. Puig-Saus, E.H. Quist, B.J. Raphael, S.J. Salipante, D.S. Shin, E. Shinbrot, B. Shirts, S. Shukla, J.L. Stanford, W. Sun, J. Tsoi, A. Upfill-Brown, D.A. Wheeler, C.J. Wu, M. Yu, S.H. Zaidi, J.M. Zaretsky, S.B. Gabriel, E.S. Lander, L.A. Garraway, T.J. Hudson, C.S. Fuchs, A. Ribas, S. Ogino, U. Peters, Genetic mechanisms of immune evasion in colorectal cancer, Cancer Discov. 8 (6) (2018) 730–749, doi:10.1158/2159-8290.CD-17-1327.

[24] S. Alfieri, S. Cavalieri, L. Licitra, Immunotherapy for recurrent/metastatic head and neck cancer, Curr. Opin. Otolaryngol. Head Neck Surg. 26 (2) (2018) 152–156, doi:10.1097/MOO.0000000000000448.

[25] S. Watanabe, J. Tanaka, T. Ota, R. Kondo, H. Tanaka, H. Kagamu, K. Ichikawa, J. Koshio, J. Baba, T. Miyabayashi, I. Narita, H. Yoshizawa, Clinical responses to EGFR-tyrosine kinase inhibitor retreatment in non-small cell lung cancer patients who benefited from prior effective gefitinib therapy: a retrospective analysis, BMC Cancer 11 (1) (2011) 1–7, doi:10.1186/1471-2407-11-1.

[26] R. Pirker, J.R. Pereira, J. Von Pawel, M. Krzakowski, R. Ramlau, K. Park, F. de Marinis, W.E. Eberhardt, L. Paz-Ares, S. Störkel, K.M. Schumacher, A. von Heydebreck, I. Celik, K.J. O'Byrne, EGFR expression as a predictor of survival for first-line chemotherapy plus cetuximab in patients with advanced non-small-cell lung cancer: analysis of data from the phase 3 FLEX study, Lancet Oncol. 13 (1) (2012) 33–42, doi:10.1016/S1470-2045(11)70318-7.

[27] P. Sharma, J.P. Allison, The future of immune checkpoint therapy, Science 348 (6230) (2015) 56–61, doi:10.1126/science.aaa8172.

[28] K.C. Shih, H. Arkenau, J.R. Infante, Clinical impact of checkpoint inhibitors as novel cancer therapies, Drugs 74 (17) (2014) 1993–2013, doi:10.1007/s40265-014-0305-6.

[29] I. Koopmans, D. Hendriks, D.F. Samplonius, R.J.V. Ginkel, S. Heskamp, P.J. Wierstra, E. Bremer, W. Helfrich, A novel bispecific antibody for EGFR-directed blockade of the PD-1/PD-L1 immune checkpoint, OncoImmunology 7 (8) (2018) 1466016, doi:10.1080/2162402X.2018.1466016.

[30] S.L. Harwood, A. Alvarezcienfuegos, N. Nunezprado, M. Compte, S. Hernandezperez, N. Merino, J. Bonet, R. Navarro, P.M.P. Van Bergen En Henegouwen, S. Lykkemark, K. Mikkelsen, K. Mølgaard, F. Jabs, L. Sanz, F.J. Blanco, P. Roda-Navarro, L. Alvarez-Vallina, ATTACK, a novel bispecific T cell-recruiting antibody with trivalent EGFR binding and monovalent CD3 binding for cancer immunotherapy, OncoImmunology 7 (1) (2018) e1377874, doi:10.1080/2162402X.2017.1377874.

[31] X.Y. Hu, R. Wang, J. Jin, X.J. Liu, A.L. Cui, L.Q. Sun, Y.P. Li, Y. Li, Y.C. Wang, Y.S. Zhen, Q.F. Miao, Z.R. Li, An EGFR-targeting antibody–drug conjugate LR004-VC-MMAE: potential in esophageal squamous cell carcinoma and other malignancies, Mol. Oncol. 13 (2) (2019) 246–263, doi:10.1002/1878-0261.12400.

[32] P. Sharma, J.P. Allison, Immune checkpoint targeting in cancer therapy: toward combination strategies with curative potential, Cell 161 (2) (2015) 205–214, doi:10.1016/j.cell.2015.03.030.

[33] R. Zappasodi, T. Merghoub, J.D. Wolchok, Emerging concepts for immune checkpoint blockade-based combination therapies, Cancer Cell 33 (4) (2018) 581–598, doi:10.1016/j.ccell.2018.03.005.

[34] S.X. Chen, L.L. Li, F. Zhang, Y. Wang, Y. Hu, L. Zhao, Immunoglobulin gamma-like therapeutic bispecific antibody formats for tumor therapy, J. Immunol. Res. 2019 (2019) 4516041, doi:10.1155/2019/4516041.

[35] S.K. Blick, L.J. Scott, Cetuximab: a review of its use in squamous cell carcinoma of the head and neck and metastatic colorectal cancer, Drugs 67 (17) (2007) 2585–2607, doi:10.2165/00003495-200767170-00008.

[36] G. Trinchieri, Interleukin-12 and the regulation of innate resistance and adaptive immunity, Nat. Rev. Immunol. 3 (2) (2003) 133–146, doi:10.1038/nri1001.

[37] C.L. Vogel, M.A. Cobleigh, D Tripathy, J.C. Gutheil, L.N. Harris, L. Fehrenbacher, D.J. Slamon, M. Murphy, W.F. Novotny, M. Burchmore, S. Shak, S.J. Stewart, M. Press, Efficacy and safety of trastuzumab as a single agent in first-line treatment of HER2-overexpressing metastatic breast cancer, J. Clin. Oncol. 20 (2002) 719–726, doi:10.1200/JCO.20.3.719.

[38] E.A. Akbay, S. Koyama, J. Carretero, A. Altabef, J.H. Tchaicha, C.L. Christensen, O.R. Mikse, A.D. Cherniack, E.M. Beauchamp, T.J. Pugh, M.D. Wilkerson, P.E. Fecci, M. Butaney, J.B. Reibel, M. Soucheray, T.J. Cohoon, P.A. Janne, M. Meyerson, D.N. Hayes, G.I. Shapiro, T. Shimamura, L.M. Sholl, S.J. Rodig, G.J. Freeman, P.S. Hammerman, G. Dranoff, K.K. Wong, Activation of the PD-1 pathway contributes to immune escape in EGFR-driven lung tumors, Cancer Discov. 3 (12) (2013) 1355–1363, doi:10.1158/2159-8290.CD-13-0310.

[39] D.I. Gabrilovich, H.L. Chen, K.R. Girgis, H.T. Cunningham, G.M. Meny, S. Nadaf, D. Kavanaugh, D.P. Carbone, Production of vascular endothelial growth factor by human tumors inhibits the functional maturation of dendritic cells, Nat. Med. 2 (10) (1996) 1096–1103, doi:10.1038/nm1096-1096.

[40] S. Trivedi, F. Conchabenavente, R.M. Srivastava, H. Jie, S.P. Gibson, N.C. Schmitt, R.L. Ferris, Immune biomarkers of anti-EGFR monoclonal antibody therapy, Ann. Oncol. 26 (1) (2015) 40–47, doi:10.1093/annonc/mdu156.

[41] S.A. Duffy, J.M. Taylor, J.E. Terrell, M. Islam, Y. Li, K.E. Fowler, G.T. Wolf, T.N. Teknos, Interleukin-6 predicts recurrence and survival among head and neck cancer patients, Cancer 113 (4) (2008) 750–757, doi:10.1002/cncr.23615.

[42] A. Yang, E.C. Lattime, Tumor-induced interleukin 10 suppresses the ability of splenic dendritic cells to stimulate CD4 and CD8 T-Cell Responses, Cancer Res. 63 (9) (2003) 2150–2157, doi:10.1097/00130404-200305000-00010.

[43] D.M. Zaiss, J. Van Loosdregt, A. Gorlani, C.P.J. Bekker, A. Grone, M. Sibilia, P.M. van Bergen en Henegouwen, R.C. Roovers, P.J. Coffer, A.J. Sijts, Amphiregulin enhances regulatory T cell-suppressive function via the epidermal growth factor receptor, Immunity 38 (2) (2013) 275–284, doi:10.1016/j.immuni.2012.09.023.

[44] A. Pivarcsi, A. Muller, A. Hippe, J. Rieker, A.V. Lierop, M. Steinhoff, S. Seeliger, R. Kubitza, U. Pippirs, S. Meller, P.A. Gerber, R. Liersch, E. Buenemann, E. Sonkoly, U. Wiesner, T.K. Hoffmann, L. Schneider, R. Piekorz, E. Enderlein, J. Reifenberger, U.P. Rohr, R. Haas, P. Boukamp, I. Haase, B. Nürnberg, T. Ruzicka, A. Zlotnik, B. Homey, Tumor immune escape by the loss of homeostatic chemokine expression, PNAS 104 (48) (2007) 19055–19060, doi:10.1073/pnas.0705673104.

[45] W. Ma, F. Conchabenavente, S.J. Santegoets, M.J.P. Welters, L. Ehsan, R.L. Ferris, S. H.Van Der Burg, EGFR signaling suppresses type 1 cytokine-induced T-cell attracting chemokine secretion in head and neck cancer, PLoS One 13 (9) (2018) e0203402, doi:10.1371/journal.pone.0203402.

[46] S. Yu, D. Liu, B. Shen, M. Shi, J.F. Feng, Immunotherapy strategy of EGFR mutant lung cancer, Am. J. Cancer Res. 8 (10) (2018) 2106–2115 PMCID: PMC6220136.

[47] J. Li, N.J. Stagg, J. Johnston, M.J. Harris, S.A. Menzies, D. Dicara, V. Clark, M. Hristopoulos, R. Cook, D. Slaga, R. Nakamura, L. McCarty, S. Sukumaran, E. Luis, Z. Ye, T.D. Wu, T. Sumiyoshi, D. Danilenko, G.Y. Lee, K. Totpal, D. Ellerman, I. Hötzel, J.R. James, T.T. Junttila, Membrane-proximal epitope facilitates efficient T cell synapse formation by anti-FcRH5/CD3 and is a requirement for myeloma cell killing, Cancer Cell 31 (3) (2017) 383–395, doi:10.1016/j.ccell.2017.02.001.

[48] C. Gerdes, V.G. Nicolini, S. Herter, E.V. Puijenbroek, S. Lang, M. Roemmele, E. Moessner, O. Freytag, T. Friess, C.H. Ries, B. Bossenmaier, H.J. Mueller, P. Umaña, GA201 (RG7160): a novel, humanized, glycoengineered anti-EGFR antibody with enhanced ADCC and superior in vivo efficacy compared with cetuximab, Clin. Cancer Res. 19 (5) (2013) 1126–1138, doi:10.1158/1078-0432.CCR-12-0989.

[49] S Li, R Schmitz K, D Jeffrey P, W Wiltzius J J, P Kussie, M Ferguson K, Structural basis for inhibition of the epidermal growth factor receptor by cetuximab, Cancer Cell 7 (4) (2005) 301–311.

[50] H. Benonisson, I. Altıntaş, M. Sluijter, S. Verploegen, A.F. Labrijn, D.H. Schuurhuis, M.A. Houtkamp, J.S. Verbeek, J. Schuurman, T. van Hall, CD3-bispecific antibody therapy turns solid tumors into inflammatory sites but does not install protective memory, Mol. Cancer Therapeutics 18 (2) (2019) 312–322, doi:10.1158/1535-7163.MCT-18-0679.